Control over the Optical and Morphological Properties of UV-Deposited Porphyrin Structures

Giovanna De Luca,[†] Gianmichele Pollicino,[†] Andrea Romeo,[†] Salvatore Patanè,[‡] and Luigi Monsù Scolaro*,[†]

Dipartimento di Chimica Inorganica, Chimica Analitica e Chimica Fisica and C.I.R.C.M.S.B., Università di Messina, Salita Sperone 31, 98166 Vill. S. Agata, Messina, Italy, and Dipartimento di Fisica della Materia e Metodologie Fisiche Avanzate, Università di Messina, via Salita Sperone No. 31, 98166 Vill. S. Agata, Messina, Italy

Received April 18, 2006. Revised Manuscript Received August 31, 2006

UV irradiation of porphyrin solutions in halogenated solvents leads to various extents of protonation, aggregation, and formation of solid deposits depending on the nature of the specific porphyrin, the light source, the initial solution concentration, the halogenated solvent, and the nature of the supporting substrate. In order to evaluate the role of various factors in controlling the main characteristics of the deposited samples, we investigated the behavior of a series of *meso*-substituted aryl porphyrins bearing protonable pyridyl peripheral groups [i.e., tetrakis(pyridyl)porphyrin isomers (*ortho* TpyP(2), *meta* TpyP(3), and *para* TpyP(4))] or hydroxyl peripheral groups [i.e., tetrakis(4-hydroxyphenyl)porphyrin (THPP) and tetrakis(3,5-dihydroxyphenyl)porphyrin (OHPP) together with some metal derivatives (Zn(II)TpyP(4) and Mn(III)TpyP(4))]. In pulsed irradiation experiments, the size and morphology of the resulting porphyrin particles strongly depend on the single pulse duration, the total irradiation time and the delay between pulses. Size and dispersity of the samples can be controlled through a careful choice of the light source (pulsed deuterium lamp or He−Cd laser). The photogenerated HX halogen acid plays an important role in modulating the optical properties (UV/vis absorption and fluorescence emission) of the porphyrin particles. The protonation and ion-pairing (for TpyPs porphyrins) and the hydrogen-bonding properties (for THPP and OHPP) together with electrostatics contribute to stabilize the growing particles at the interface between the solution and the supporting surface. The possibility of controlling the size of the deposited particles in the nanoscopic range (100−200 nm) has been demonstrated.

Introduction

Supramolecular assemblies of porphyrins are of particular interest for their applications as model systems in the conversion and storage of solar energy[1] or in materials chemistry.[2] Indeed, besides the covalent approach,[3] self-assembly based on weak interactions seems to be a promising alternative since it is synthetically less demanding to obtain organized multi-chromophoric arrays. Thus, the use of porphyrin derivatives bearing groups capable of supramolecular interactions can be a viable method to assemble such organized structures.[4] Among *meso*-substituted porphyrins, pyridyl or hydroxyphenyl functionalized molecules are particularly appealing for their coordination and hydrogen-bonding abilities, which can work together with electrostatics and dispersive forces to organize the chromophores in the aggregates. By metal-directed self-assembly, pyridyl functionalized porphyrins can be used as building blocks to obtain three-dimensional frameworks[5] and discrete nanosized structures,[6] some of which are also able to participate in hierarchically organized assemblies.[7] Furthermore, the for-

* Corresponding author. Phone: +39 090 676 5711. Fax: +39 090 393756. E-mail: lmonsu@unime.it.

[†] Dipartimento di Chimica Inorganica, Chimica Analitica e Chimica Fisica and C.I.R.C.M.S.B.

[‡] Dipartimento di Metodologie Fisiche Avanzate.

(1) (a) Wasielewski, M. R. *Chem. Rev.* **1992**, *92*, 435. (b) Kurreck, H.; Huber, M. *Angew. Chem., Int. Ed. Engl.* **1995**, *34*, 849.

(2) (a) Chou, J.-H.; Kosal, M. E.; Nalwa, H. S.; Suslick, K. S. In *The Porphyrin Handbook*; Kadish, K., Smith, K., Guilard, R., Eds.; Academic Press: New York, 2000; Vol. 6, p 43. (b) Burrell, A. K.; Wasielewski, M. R. *J. Porphyrins Phthalocyanines* **2000**, *4*, 401. (c) Suslick, K. S.; Rakow, N. A.; Kosal, M. E.; Chou, J.-H. *J. Porphyrins Phthalocyanines* **2000**, *4*, 407. (d) Drain, C. M.; Hupp, J. T.; Suslick, K. S.; Wasielewski, M. R.; Chen, X. *J. Porphyrins Phthalocyanines* **2002**, *6*, 243.

(3) (a) Li, J.; Ambroise, A.; Yang, S. I.; Diers, J. R.; Seth, J.; Wack, C. R.; Bocian, D. F.; Holten, D.; Lindsey, J. S. *J. Am. Chem. Soc.* **1999**, *121*, 8927. (b) Burrell, A. K.; Officer, D. L.; Plieger, P. G.; Reid, D. C. W. *Chem. Rev.* **2001**, *101*, 2751.

(4) Chambron, J.-C.; Heitz, V.; Sauvage, J.-P. In *The Porphyrin Handbook*; Kadish, K., Smith, K., Guilard, R., Eds.; Academic Press: New York, 2000; Vol. 6, p 1.

(5) (a) Qian, D.-J.; Nakamura, C.; Ishida, T.; Wenk, S.-O.; Wakayama, T.; Takeda, S.; Miyake, J. *Langmuir* **2002**, *18*, 10237. (b) Goldberg, I. *Chem. Commun.* **2005**, 1243.

(6) (a) Drain, C. M.; Nifiatis, F.; Vasenko, A.; Batteas, J. D. *Angew. Chem., Int. Ed.* **1998**, *37*, 2344. (b) Huck, W. T. S.; Rohrer, A.; Anilkumar, A. T.; Fokkens, R. H.; Nibbering, N. M. M.; van Veggel, F.; Reinhoudt, D. N. *New J. Chem.* **1998**, *22*, 165. (c) Leininger, S.; Olenyuk, B.; Stang, P. J. *Chem. Rev.* **2000**, *100*, 853. (d) Iengo, E.; Zangrando, E.; Minatel, R.; Alessio, E. *J. Am. Chem. Soc.* **2002**, *124*, 1003. (e) Iengo, E.; Zangrando, E.; Alessio, E. *Eur. J. Inorg. Chem.* **2003**, 2371.

(7) (a) Schenning, A.; Benneker, F. B. G.; Geurts, H. P. M.; Liu, X. Y.; Nolte, R. J. M. *J. Am. Chem. Soc.* **1996**, *118*, 8549. (b) Hofkens, J.; Latterini, L.; Vanoppen, P.; Faes, H.; Jeuris, K.; DeFeyter, S.; Kerimo, J.; Barbara, P. F.; DeSchryver, F. C.; Rowan, A. E.; Nolte, R. J. M. *J. Phys. Chem. B* **1997**, *101*, 10588. (c) Milic, T. N.; Chi, N.; Yablon, D. G.; Flynn, G. W.; Batteas, J. D.; Drain, C. M. *Angew. Chem., Int. Ed.* **2002**, *41*, 2117. (d) Lensen, M. C.; Castriciano, M.; Coumans, R. G. E.; Foekema, J.; Rowan, A. E.; Scolaro, L. M.; Nolte, R. J. M. *Tetrahedron Lett.* **2002**, *43*, 9351.

10.1021/cm060896s CCC: $33.50
Published on Web 10/12/2006

mation of nanoparticles,[8] gels,[9] Langmuir−Blodgett films,[10] and self-assembled monolayers of covalently[11] and noncovalently[12] bound pyridylporphyrins have also been reported. Various examples of structured aggregates also exist in the literature for hydroxyphenyl-substituted porphyrins, which are able to form solid networks[13] and ultrathin films for nonlinear optics applications.[14]

Recently, we reported some preliminary results on the possibility of forming solid porphyrin deposits by simply irradiating dichloromethane solutions of these chromophores with UV light. In particular, upon repeated irradiation of a tetrakis(4-pyridyl)porphyrin (TpyP(4)) dichloromethane solution with the lamp of an UV/vis diode array spectrophotometer, the formation of a deposit was observed in a quartz cell on the surface exposed to the light beam.[15] Furthermore, the deposition of a porphyrin thin film exhibiting acid−base sensing properties has been obtained on irradiating dichloromethane solutions of the tetrabutylammonium salt of tetrakis(4-sulfonatophenyl)porphyrin (TPPS).[16]

Here we describe a systematic investigation carried out on various pyridyl and hydroxyphenyl porphyrins (Scheme 1) to elucidate the critical parameters that control the UV-induced deposition process. The dependence of the morphology and optical properties of various deposited samples will be discussed as a function of the nature of (i) the porphyrin peripheral substitution, (ii) the surface used as support for the samples, and (iii) the halogenated solvent. In addition, the possibility to exert control over the size of the deposited objects will be demonstrated.

Experimental Section

Chemicals. *meso*-Tetrakis(4-pyridyl)porphyrin (TpyP(4)) and *meso*-tetrakis(4-hydroxyphenyl)porphyrin (THPP) were purchased from Aldrich Chemical Co., while *meso*-tetrakis(3,5-dihydroxyphenyl)porphyrin (OHPP) was purchased from Tokyo Kasey Kogyo Co., Ltd. These products were used as received without further purification. *meso*-Tetraphenylporphyrin (TPP), *meso*-tetrakis(2-pyridyl)porphyrin (TpyP(2)), *meso*-tetrakis(3-pyridyl)porphyrin (TpyP(3)), and *meso*-tetrakis(4-methoxyphenyl)porphyrin (TMPP) as well as Zn(II) and Mn(III) derivatives of TpyP(4) were prepared according to literature procedures.[17,18] Solutions of these porphyrins were generally prepared in spectrophotometric grade dichloromethane (Sigma), with the addition of a few drops of spectrophotometric grade methanol (Aldrich; 2% v/v) in the case of Zn(II)TpyP(4), THPP and OHPP, to increase their solubility. All other chemicals were of the highest grade available (Aldrich) and were used as received.

Scheme 1. Molecular Structures of the Investigated Porphyrins

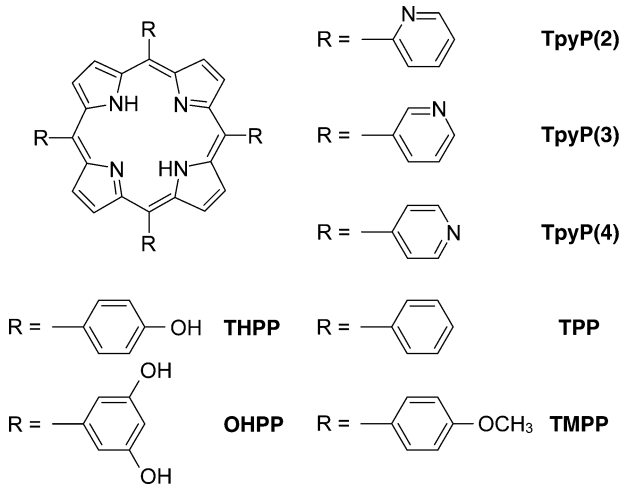

Stock solutions were stored in the dark and used within 1 week of preparation. The range of concentration (5−10 μM) used in our experiments was determined spectrophotometrically using the molar extinction coefficients at the Soret maxima [TpyP(4): 4.54×10^5 $M^{-1}\cdot cm^{-1}$, $\lambda = 416$ nm; TpyP(3): 5.59×10^5 $M^{-1}\cdot cm^{-1}$, $\lambda = 419$ nm; TpyP(2): 3.49×10^5 $M^{-1}\cdot cm^{-1}$, $\lambda = 417$ nm; TPP: 4.78×10^5 $M^{-1}\cdot cm^{-1}$, $\lambda = 418$ nm; TMPP: 4.57×10^5 $M^{-1}\cdot cm^{-1}$, $\lambda = 420$ nm; THPP: 4.57×10^5 $M^{-1}\cdot cm^{-1}$, $\lambda = 421$ nm; OHPP: 2.95×10^5 $M^{-1}\cdot cm^{-1}$, $\lambda = 419$ nm],[18−20] except for the two TpyP(4) metal derivatives, in which cases saturated solution were employed.

Spectroscopic Methods. UV/vis extinction spectra were recorded on Hewlett-Packard diode-array spectrophotometers (model HP 8452A and HP 8453). Steady-state fluorescence (emission and excitation) and resonance light-scattering (RLS) experiments were performed on a Jasco model FP-750 spectrofluorimeter equipped with a Hamamatsu R928 photomultiplier. For RLS experiments, a synchronous scan protocol with a right-angle geometry was adopted.[21] When necessary, a UV filter (Hoya glass type UV-34, cutoff: 340 nm) was used in order to cut off the UV component of the spectrophotometer lamp and avoid the formation of haloacids by photodecomposition of the halogenated solvent. Fluorescence and RLS spectra were not corrected for absorption of the samples.

Microscopy Techniques. Optical microscopy images were obtained with a Zeiss Axiovert S100 microscope equipped with Plan Neofluar objectives (10×, n.a. = 0.3; 50×, n.a. = 0.5, long working distance). Atomic force microscopy images were obtained by using a ThermoMicroscopes model Explorer AFM working in contact mode.

Secondary electron microscopy (SEM) analyses were performed on a JEOL JSM/5600 LV instrument operating with an accelerating potential of 20 kV. Samples were prepared by gold coating.

(8) (a) Gong, X.; Milic, T.; Xu, C.; Batteas, J. D.; Drain, C. M. *J. Am. Chem. Soc.* **2002**, *124*, 14290. (b) Drain, C. M.; Bazzan, G.; Milic, T.; Vinodu, M.; Goeltz, J. C. *Isr. J. Chem.* **2005**, *45*, 255.
(9) Tanaka, S.; Shirakawa, M.; Kaneko, K.; Takeuchi, M.; Shinkai, S. *Langmuir* **2005**, *21*, 2163.
(10) Kroon, J. M.; Sudholter, E. J. R.; Schenning, A.; Nolte, R. J. M. *Langmuir* **1995**, *11*, 214.
(11) (a) Li, D.; Swanson, B.; Robinson, J. M.; Hoffbauer, M. A. *J. Am. Chem. Soc.* **1993**, *115*, 6975. (b) Yerushalmi, R.; Scherz, A.; vanderBoom, M. E. *J. Am. Chem. Soc.* **2004**, *126*, 2700.
(12) (a) Van Galen, D. A.; Majda, M. *Anal. Chem.* **1988**, *60*, 1549. (b) Sharma, C. V. K.; Broker, G. A.; Szulczewski, G. J.; Rogers, R. D. *Chem. Commun.* **2000**, 1023. (c) He, Y.; Ye, T.; Borguet, E. *J. Am. Chem. Soc.* **2002**, *124*, 11964.
(13) (a) Goldberg, I.; Krupitsky, H.; Stein, Z.; Hsiou, Y.; Strouse, C. E. *Supramol. Chem.* **1994**, *4*, 203. (b) Bhyrappa, P.; Wilson, S. R.; Suslick, K. S. *J. Am. Chem. Soc.* **1997**, *119*, 8492. (c) Bhyrappa, P.; Wilson, S. R.; Suslick, K. S. *Supramol. Chem.* **1998**, *9*, 169. (d) Suslick, K. S.; Bhyrappa, P.; Chou, J.-H.; Kosal, M. E.; Nakagaki, S.; Smithenry, D. W.; Wilson, S. R. *Acc. Chem. Res.* **2005**, *38*, 283.
(14) Jiang, L.; Lu, F.; Li, H.; Chang, Q.; Li, Y.; Liu, H.; Wang, S.; Song, Y.; Cui, G.; Wang, N.; He, X.; Zhu, D. *J. Phys. Chem. B* **2005**, *109*, 6311.
(15) Scolaro, L. M.; Romeo, A.; Castriciano, M. A.; De Luca, G.; Patanè, S.; Micali, N. *J. Am. Chem. Soc.* **2003**, *125*, 2040.
(16) De Luca, G.; Pollicino, G.; Romeo, A.; Scolaro, L. M. *Chem. Mater.* **2006**, *18*, 2005.
(17) (a) Adler, A. D.; Longo, F. R.; Finarelli, J. D.; Goldmacher, J.; Assour, J.; Korsakoff, L. *J. Org. Chem.* **1967**, *32*, 476. (b) Adler, A. D.; Longo, F. R.; Kampas, F.; Kim, J. *J. Inorg. Nucl. Chem.* **1970**, *32*, 2443.
(18) Kalyanasundaram, K. *Inorg. Chem.* **1984**, *23*, 2453.
(19) Stone, A.; Fleischer, E. B. *J. Am. Chem. Soc.* **1968**, *90*, 2735.
(20) Bonar-Law, R. P. *J. Org. Chem.* **1996**, *61*, 3623.
(21) Pasternack, R. F.; Collings, P. J. *Science* **1995**, *269*, 935.

Scanning near-field optical luminescence (SNOL) measurements were performed by means of a "homemade" aperture microscope in excitation mode configuration.[22] The instrument was operating in constant gapwidth mode (CGM) stabilizing the distance between the sample and the tip by a tuning fork based non optical shear-force mechanism.[23] The near field was provided by coupling an Ar^+ laser emitting at 488 nm coupled to a commercially available tapered optical fiber (Nanonix) with a 50 nm wide nominal aperture. Because of the features of the technique, namely, super resolution and room condition working capability, the samples were observed as obtained after the deposition. Measurements were performed with a scan rate of about 12 nm/min and a sampling of 256 point/row. Optical and topographic data were simultaneously collected during the scans and stored in a personal computer for further analysis.

Images analyses were performed by the SigmaScan Pro 5.0 software from Systat Software Inc., Richmond, CA.

Deposition Methods. To obtain deposited samples on silica, a quartz cuvette containing the porphyrin solution ([porphyrin] $\sim$ 5−10 μM) was cyclically exposed to the UV light by controlling the shutter of the diode-array spectrophotometer. Typical values for irradiation time (i.t.) can vary between 0.1 and 0.5 s, while the delay time (d.t.) can assume values ranging from 5 to 15 s, both values depending on the efficiency of the spectrophotometer lamp. The total irradiation time (t.t.) depends on how many irradiations have to be performed and may range from 200 to 6000 s.

To obtain TpyP(4) deposits on different surfaces and to produce samples suitable for SEM, SNOM, and AFM analyses, small slides of silica (cleaned by immersion in a basic piraña solution, thoroughly rinsed with bidistilled water and finally dried under N_2) and gold- or aluminum-coated silicon were inserted in a quartz cell filled with porphyrin solution. A 10 mW He/Cd laser (325 nm line) was then used as a continuous UV light source. When beam attenuation was necessary, a neutral density filter (0.5 AU) was employed.

In all the deposition experiments, the porphyrin excess was removed by washing the solid samples with neat halogenated solvent.

Results and Discussion

Irradiation Experiments. TpyP(4) is soluble in dichloromethane, and its solutions display spectral features that are commonly observed for monomeric porphyrins: (i) an intense Soret band (416 nm) accompanied by four weaker Q-bands at longer wavelengths in UV/vis spectra, (ii) a strong two-banded fluorescence, and (iii) a weak RLS profile characterized by a trough due to photon absorption at the wavelength of the Soret band. On repeated scanning of this solution with a UV/vis diode-array spectrophotometer (i.t., 0.5 s; d.t., 5 s; t.t., 3900 s; under stirring), large changes are observed in the extinction spectrum, as shown in Figure 1a. The starting Soret band decreases in intensity, and a new band appears at longer wavelengths (485 nm); these changes being accompanied by a baseline rise and some changes in the Q-bands ratios.

The spectra of the irradiated solution display extremely broad features, and no isosbestic points can be detected in the spectral changes occurring upon irradiation. The fluorescence emission of the final solution is almost totally quenched, and the corresponding RLS spectrum displays an intense feature at the red edge of the Soret band (Figure 1b,c). The comparison of this evidence with the results reported in the literature for the aggregation processes involving the acid derivatives of TpyP isomers[24] suggests the formation of hexaprotonated TpyP(4) aggregates upon irradiation.

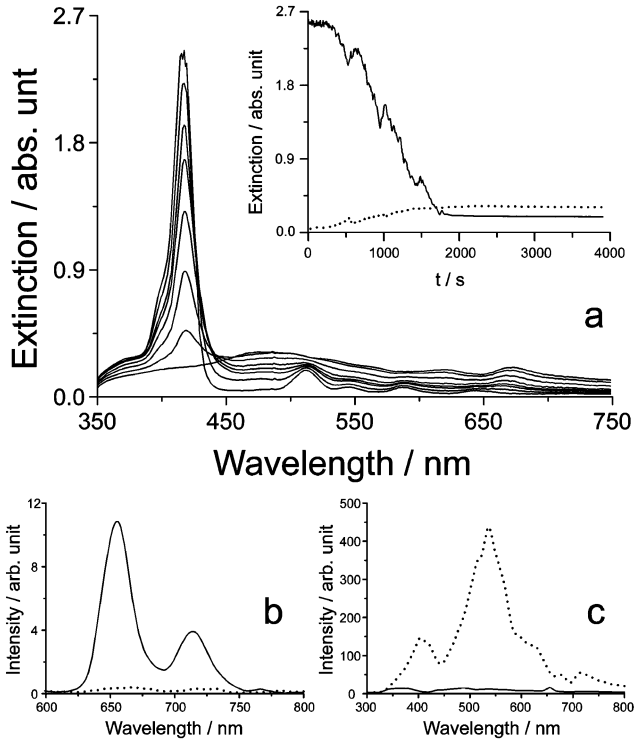

Figure 1. (a) Changes in the extinction spectra occurring upon irradiation of a TpyP(4) solution in CH_2Cl_2 with a spectrophotometer lamp. [TpyP(4)] = 6 μM; i.t. = 0.5 s; d.t. = 5 s; t.t. = 3900 s; under stirring. Inset: changes observed at 416 nm (solid line) and 485 nm (dotted line). (b and c) Fluorescence and RLS spectra, respectively, of the solution before (solid line) and after (dotted line) irradiation.

When the same experiments are performed on tetraphenylporphyrin (TPP) dichloromethane solutions, the free base is converted to its monomeric diacid derivative, ion-paired with the chloride anion, as indicated by[25] (i) the sharp Soret band of the irradiated solution is found at a longer wavelength (446 nm) than TPP (418 nm) and is accompanied by three Q-bands; (ii) both fluorescence profile and position are strongly influenced by protonation, the emission being still intense; and (iii) the RLS signals are comparable to those of the starting solution (Supporting Information).

These observations suggest that a non-negligible photodecomposition of the chlorinated solvent can occur during the irradiation with the UV light from the spectrophotometer,[26] leading to the production of hydrochloric acid and, thus, to the formation of the various porphyrin acid derivatives. A series of experiments have been carried out to further

(22) (a) Gucciardi, P. G.; Labardi, M.; Gennai, S.; Lazzeri, F.; Allegrini, M. *Rev. Sci. Instrum.* **1997**, *68*, 3088. (b) Labardi, M.; Gucciardi, P. G.; Allegrini, M. *Riv. Nuovo Cimento* **2000**, *23*, 1.
(23) (a) Betzig, E.; Finn, P. L.; Weiner, J. S. *Appl. Phys. Lett.* **1992**, *60*, 2484. (b) Grober, R. D.; Harris, T. D.; Trautman, J. K.; Betzig, E. *Rev. Sci. Instrum.* **1994**, *65*, 626. (c) Karrai, K.; Grober, R. D. *Ultramicroscopy* **1995**, *61*, 197−205.
(24) De Luca, G.; Romeo, A.; Scolaro, L. M. *J. Phys. Chem. B* **2005**, *109*, 7149.
(25) Rosa, A.; Ricciardi, G.; Baerends, E. J.; Romeo, A.; Scolaro, L. M. *J. Phys. Chem. A* **2003**, *107*, 11468.
(26) Weissberger, A.; Proskauer, E. S. *Organic Solvents: Physical Properties and Methods of Purification*; Interscience Publishers, Inc.: New York, 1955; Vol. 7, p 409.

verify this conclusion. First, small quantities of triethylamine vapors have been added to the irradiated porphyrins solutions, leading to the conversion of their spectral features to those of the starting free bases. Second, irradiation of neat CH_2Cl_2 has been performed to rule out the possibility that the porphyrins are acting as sensitizers for the solvent decomposition. In this case, the effective formation of HCl has been revealed by adding to the irradiated CH_2Cl_2 small quantities of TPP as an indicator, the color of the solution turning to the typical green of the corresponding porphyrin diacid. Third, the previously described behavior has also been observed for irradiated porphyrins solutions in chloroform, whereas no changes have occurred by irradiating solutions in non-halogenated solvents like acetone, methanol, DMF, or DMSO.[27] Finally, in order to demonstrate that the solvent decomposition is caused by the UV component of the incident light, a high-pass filter (cutoff, 340 nm) has been used during the irradiation of a TPP solution, and no changes have been observed even after a total irradiation time of 6000 s.

TpyP(4) Deposition Experiments. If the irradiation of a TpyP(4) dichloromethane solution ([TpyP(4)] $\sim 5-10\ \mu$M) is performed without stirring and under conditions of short i.t. (0.1−0.3 s) and long d.t. (≥10 s; t.t. = 6000 s), the formation of a spot having the shape of the light beam section can be observed on the internal surface of the cell at the end of the experiment (Supporting Information). Under these conditions, the photogenerated acid is not dispersed in solution, and its local concentration at the illuminated quartz/solvent interface nearer to the UV light source remains quite low. This allows the concentration of the protonated porphyrin to increase locally, thus causing this species to slowly accumulate as a solid on the cell surface due to its low solubility in dichloromethane. After removing the irradiated solution from the quartz cell, the deposit can be rinsed with neat dichloromethane several times without being dissolved. Deposited samples have also been produced by using the 325 nm line of a 10 mW He/Cd laser as a continuous UV light source (total irradiation time ranging from 4 to 24 h). A small circular spot has been obtained on both the two walls of the quartz cell along the light path, for the laser beam being only slightly absorbed by the solvent at this wavelength.

Solid samples show a broad Soret band in the extinction spectra, red-shifted with respect to that of the starting solution (Table 1 and Supporting Information), and the presence of four Q-bands suggests that the deposit consists of species that have been protonated only at the *meso* pyridyl groups. These samples are fluorescent with a two-band emission profile, and no distinctive features are found in the RLS spectra.

By carrying out deposition experiments from TpyP(4) solutions in dibromo- and diiodomethane, it is possible to point out the dependence of the spectroscopic features of the various deposits on the nature of the halogenated solvent (Table 1) (i.e., on the nature of the halogen acid that forms upon solvent photodecomposition). A similar dependence has already been pointed out in the case of the acid-induced aggregates of TpyP isomers as a consequence of the participation of the anions in stabilizing the aggregates structures.[24] Analogously, we are inclined to explain the observed variation of the optical properties of samples deposited from different halogenated solvents as a consequence of the interaction between the protonated porphyrin macrocycle and the counteranions.

(27) Acidification has also been observed with solutions prepared in CCl_4, but the presence of CH_2Cl_2 and $CHCl_3$ as impurities in this solvent does not allow us to draw any decisive conclusion.

Table 1. Spectroscopic Features of the Porphyrin Starting Solutions and the Corresponding Deposits on Silica

porphyrin	sample	Soret band (nm)	Q- bands (nm)				emission (nm)	
TpyP(4)	solution	416	513	546	589	646	653	713
	deposit	426	520	557	595	661	664	711
	deposit[a]	438	538	570	610	664	676[b]	713[b]
	deposit[c]	448	532	602	673	762		
TpyP(3)	solution	419	515	557	595	661	664	711
	deposit	453			616	666	682	714
TpyP(2)	solution	417	513	546	588	643	649	713
	deposit	488		570	615	668		
THPP	solution	424	519	557	595	651	657	722
	deposit	486			695	773		
OHPP	solution	422	519	556	595	651	657	721
	deposit	503				791		

[a] From CH_2Br_2; an additional Soret band component is observed at 484 nm, probably due to deposition of completely protonated species. [b] Low intensity. [c] From CH_2I_2.

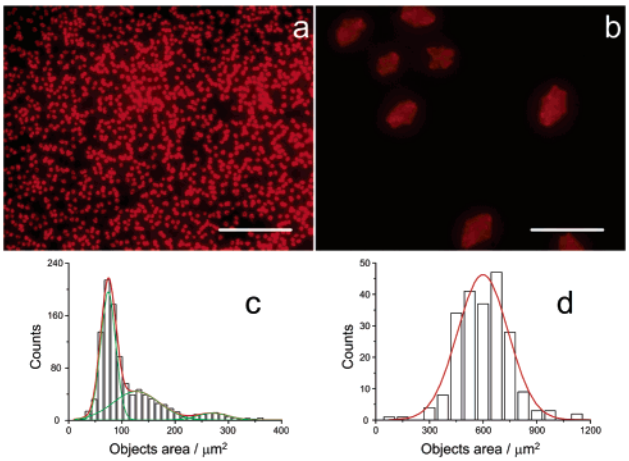

Figure 2. Optical images (a and b, fluorescence mode exciting at 532 nm) and related size distributions (c and d, respectively) of the deposits obtained by irradiating a CH_2Cl_2 solution of TpyP(4). [TpyP(4)] $\sim 6\ \mu$M; (a) UV light source: spectrophotometer lamp, i.t. = 0.3 s, d.t. = 10 s, t.t. = 3600 s; (b) UV light source: He/Cd laser, continuous irradiation, neutral density filter (0.5 AU), t.t. = 24 h. Bar: 50 μm.

The deposits have been analyzed by optical microscopy to acquire information on their morphology, and the samples obtained from the TpyP(4)/CH_2Cl_2 system appear to be made of microscopic fluorescent crystals, as shown by the optical images reported in Figure 2a,b.

The size (area) distribution of the crystals deposited by means of the spectrophotometer lamp, as obtained from image analysis, is described by three Gaussians centered around 70, 130, and 270 μm^2 (standard deviations: 28, 87, and 59 μm^2, respectively). This evidence can be explained by considering the presence of clustered objects rather than the formation of a polydispersed sample. The use of a He/Cd laser leads to deposits consisting of larger and better

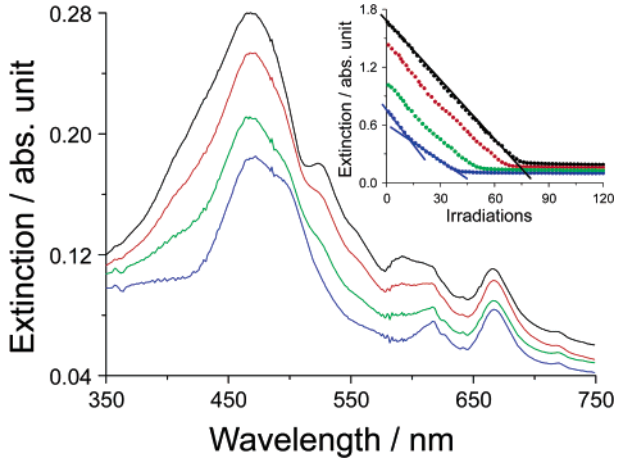

Figure 3. Extinction spectra of TpyP(4) solutions after irradiation (under stirring) by using the spectrophotometer lamp. Inset: changes occurring during the irradiation experiments, observed at 485 nm. [TpyP(4)] = 3.7 μM (black); 3.1 μM (red); 2.2 μM (green); 1.5 μM (blue). i.t. = 0.5 s; d.t = 5 s; t.t. = 1000 s.

separated crystals whose mean area is 600 μm^2 (standard deviation: 284 μm^2) with an evident monodispersity across the sample. The difference in size and dispersity can be ascribed to a slower acid photogeneration in the case of the laser UV source since (i) a laser source is nearly monochromatic, while a broad range of wavelengths are effective for solvent photodecomposition on using a deuterium lamp, and (ii) the laser wavelength (325 nm) is quite far from the UV region where dichloromethane absorption is higher (CH_2Cl_2 cutoff, 240 nm).

In order to determine the minimum concentration for TpyP(4) solutions that gives deposited samples, a series of irradiation experiments have been carried out over a range of porphyrin concentrations. Relevant information has been obtained by the extinction spectra of solutions irradiated under stirring, especially looking at the ratios between the Q-band intensities as well as from the spectral changes observed at fixed wavelength during the course of the experiments (Figure 3). These results indicate that the ratio between peripherally protonated molecules and fully protonated ones, which form simultaneously upon irradiation, decreases on decreasing the starting porphyrin concentration. The spectral changes observed at fixed wavelength are also compatible with an initial formation of the peripherally tetraprotonated porphyrins. In the case of the most dilute solutions, the tetraprotonated species come to a further protonation stage due to the lower ratio between the local concentration of TpyP(4) and that of the acid photogenerated at every light pulse.

To determine if the nature of the surface on which the deposit forms exerts any influence on the crystals morphology, some samples were deposited on different substrates such as silica, aluminum, or gold. Figure 4 reports AFM (a and b) and SEM (c and d) images for TpyP(4) samples deposited on silica- (a and c) and gold-coated silicon (b and d). Both samples are constituted by clustered pyramidal objects, but the silica surface seems to allow more extensive crystal formation with respect to the gold one,[28] suggesting a higher affinity of the tetraprotonated species that form upon irradiation for the former surface.

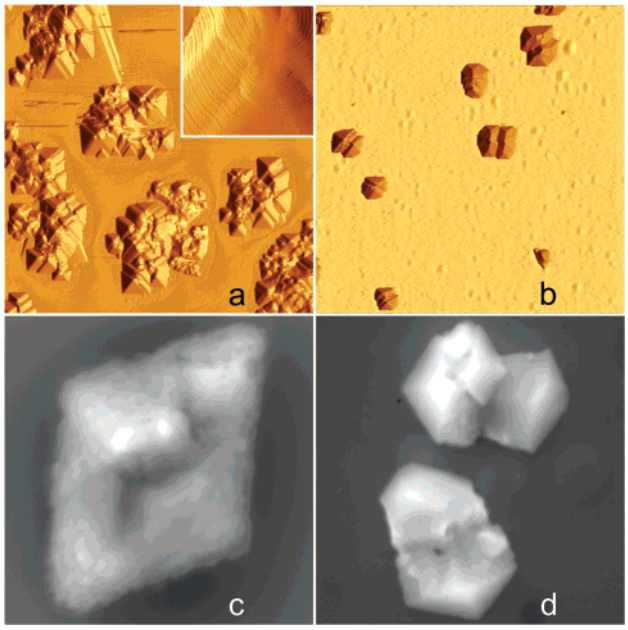

Figure 4. AFM and SEM images of TpyP(4) deposits on silica (a and c) and gold-coated silicon (b and d), obtained by continuous irradiation of porphyrin solutions with a 10 mW He/Cd laser (325 nm) in the presence of small pieces of the two surfaces across the optical pathway. (a and b) AFM images, after applying a shading filter; 50 × 50 μm^2. Inset: 1 × 1 μm^2. (c and d) SEM images; 10 × 10 μm^2. [TpyP(4)] ~ 6 μM; continuous irradiation; t.t. = 6 h.

Other Porphyrins Deposition. Experiments carried out irradiating dichloromethane solutions of TPP, which can be protonated only at the inner nitrogen atoms, do not give any evidence of deposit formation since the diacid derivative of this porphyrin is readily soluble in this solvent.[19,25] Deposited samples are however easily obtained by irradiating dichloromethane solutions of TpyP(2) and TpyP(3) porphyrins (Supporting Information). These deposits consist of microcrystals smaller than those formed in the TpyP(4) case. By comparing extinction and emission spectra of the spots obtained with the three TpyP isomers as well as the spectral changes upon irradiation in the various cases, it is possible to notice that increasing amounts of hexaprotonated species are present in the deposits in the order TpyP(4) < TPyP(3) < TpyP(2). Indeed, the number of Q-bands is reduced and quenching of fluorescence emission is observed especially for the ortho isomer. The spectral changes observed in solution on irradiation lead to the same conclusions, all this evidence being in agreement with the behavior already described for these porphyrins upon addition of HCl vapors.[24]

Other deposition experiments have been carried out on dichloromethane solutions of TpyP(4) metal derivatives to study the effect of preventing core protonation by the photogenerated acid. Figure 5 shows the optical images of the Mn(III)TpyP(4) and Zn(II)TpyP(4) deposits (a and b, respectively), showing a marked dependence of the crystals morphology on the nature of the metal ion coordinated to the inner nitrogen atoms. In particular, the Mn(III) species gives very regular square crystals with a mean dimension of approximately 100 μm^2, while the Zn(II) derivative affords

(28) The morphology of the crystals obtained over aluminium-coated silicon resembles that observed for deposits on silica.

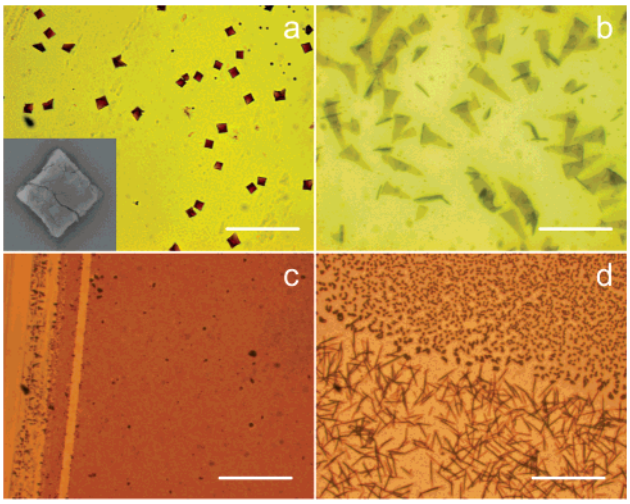

Figure 5. Optical images (transmission) of the deposits obtained by irradiating CH_2Cl_2 solutions of various porphyrins. UV light source: spectrophotometer lamp; i.t. = 0.3 s, d.t. = 10 s, t.t. = 3600 s; porphyrins concentration ~ 6 μM. (a) Mn(III)TpyP(4). Inset: SEM image, 10 × 10 μm^2. (b) Zn(II)TpyP(4). (c) THPP. (d) OHPP. Bar: 50 μm.

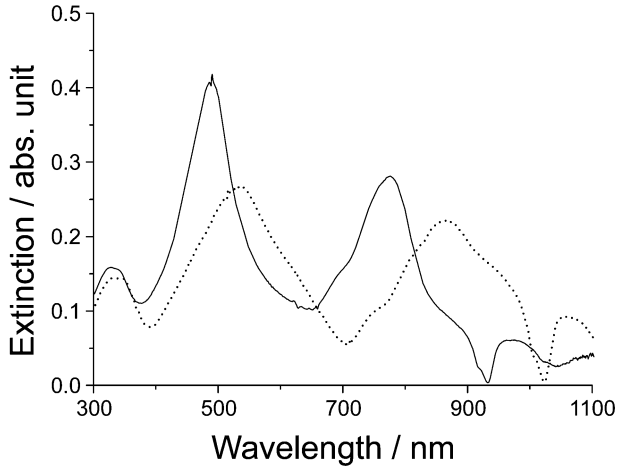

Figure 6. Extinction spectra of THPP (solid line) and OHPP (dotted line) samples deposited on quartz by pulsed irradiation with a spectrophotometer lamp. [porphyrin] ~ 6 μM, i.t. = 0.3 s, d.t. = 10 s, t.t. = 3600 s.

needle crystals from which ribbon-like structures grow toward the solution phase.[15]

Figure 5 also reports the optical images of deposited samples obtained by pulsed irradiation of dichloromethane solutions of THPP and OHPP. THPP is the only porphyrin under investigation to form a homogeneous film, as indicated by the scratched zone in Figure 5c. On the contrary, it is possible to recognize two different morphologies for the microscopic crystals that form upon irradiation of OHPP solutions: smaller and geminate crystals are present in the central part of the spot, while needle-like objects are observed at its periphery. This difference can be probably ascribed to a non-homogeneous local concentration of photogenerated HCl.[29]

The extinction spectra of both deposited samples (Figure 6) and irradiated solutions of THPP and OHPP display extremely broad features, substantially red-shifted as compared to the spectra of the corresponding starting solutions (Table 1). The Q-bands extend as far as the near-infrared and their intensities are comparable to those of the Soret bands.

These kind of spectra have been referred to as *hyperporphyrin spectra*[30] and have already been observed for various metalloporphyrins[30,31] or for monomeric acid derivatives of porphyrins having hydroxyphenyl or dimethylaminophenyl *meso* substituents.[32−34] The presence of a marked broadening and red shift of the Soret bands, accompanied by enhanced and red-shifted Q-bands, has been ascribed to charge-transfer processes either into or out of the porphyrin ring.[33,34] According to this hypothesis, the extra orbitals providing the charge-transfer level belong to the coordinated metal ion or, as in our case, to suitably conjugated substituents.[33] Recent investigations on the behavior of THPP and OHPP upon acidification of their dichloromethane solutions have pointed out that, under appropriate experimental conditions, extended J-type aggregates can form leading to extremely broadened and red-shifted extinction features.[35] In the present case, besides the hyperporphyrin character of the two chromophores, the presence of intense resonant scattering component has been considered to account for the exceptional broadening and bathochromic shift observed in the extinction spectra.[36]

A comparison of the results obtained with the different porphyrins permits some general conclusion to be drawn. First, the presence of extinction features that are red-shifted with respect to those of the starting free bases, both for solid samples and aggregates formed in solution, suggests that a J-type arrangement of the chromophores is adopted in the various structures.[37] Depending on the nature of the *meso* substituents, the structures which form upon irradiation can be stabilized by contributions of electrostatics (ion-pairing), hydrogen-bonding, and dispersive interactions. For example, in the case of J-type aggregates reported in the literature for tetraprotonated TpyP(4) acid derivatives,[24] the suggested structure also involves the (halide) anions, whose presence reduces the repulsion among positively charged porphyrin monomers and allows aggregates formation. Also in this case, the deposits spectral features depend on the nature of the counteranion, and Figure 7 suggests a model that may account for this observation, describing the interaction

(29) It is interesting to note that, upon prolonged irradiation of OHPP solutions, a complete deposition of the porphyrin occurs, as evidenced by the total decoloration of the samples.

(30) Gouterman, M. In *The Porphyrins*; Dolphin, D., Ed.; Academic Press: New York, 1978; Vol. 3, p 1.
(31) (a) Hanson, L. K.; Eaton, W. A.; Sligar, S. G.; Gunsalus, I. C.; Gouterman, M.; Connell, C. R. *J. Am. Chem. Soc.* **1976**, *98*, 2672. (b) Milgrom, L. R.; Jones, C. C.; Harrimann, A. *J. Chem. Soc., Perkin Trans. 2* **1988**, 71.
(32) Traylor, T. G.; Nolan, K. B.; Hildreth, R. *J. Am. Chem. Soc.* **1983**, *105*, 6149.
(33) Ojadi, E. C. A.; Linschitz, H.; Gouterman, M.; Walter, R. I.; Lindsey, J. S.; Wagner, R. W.; Droupadi, P. R.; Wang, W. *J. Phys. Chem.* **1993**, *97*, 13192.
(34) (a) Vitasovic, M.; Gouterman, M.; Linschitz, H. *J. Porphyrins Phthalocyanines* **2001**, *5*, 191. (b) Wasbotten, I. H.; Conradie, J.; Ghosh, A. *J. Phys. Chem. B* **2003**, *107*, 3613. (c) Guo, H.; Jiang, J.; Shi, Y.; Wang, Y.; Liu, J.; Dong, S. *J. Phys. Chem. B* **2004**, *108*, 10185.
(35) De Luca, G.; Romeo, A.; Scolaro, L. M. *J. Phys. Chem. B* **2006**, *110*, 14135−14141.
(36) Micali, N.; Mallamace, F.; Castriciano, M.; Romeo, A.; Scolaro, L. M. *Anal. Chem.* **2001**, *73*, 4958.
(37) Kobayashi, T., Ed. *J-Aggregates*; World Scientific: Singapore, 1996.

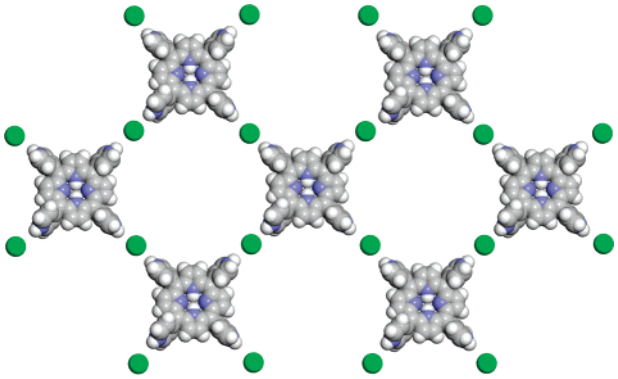

Figure 7. Schematic model of the TpyP(4) deposit, the green spheres representing halide anions.

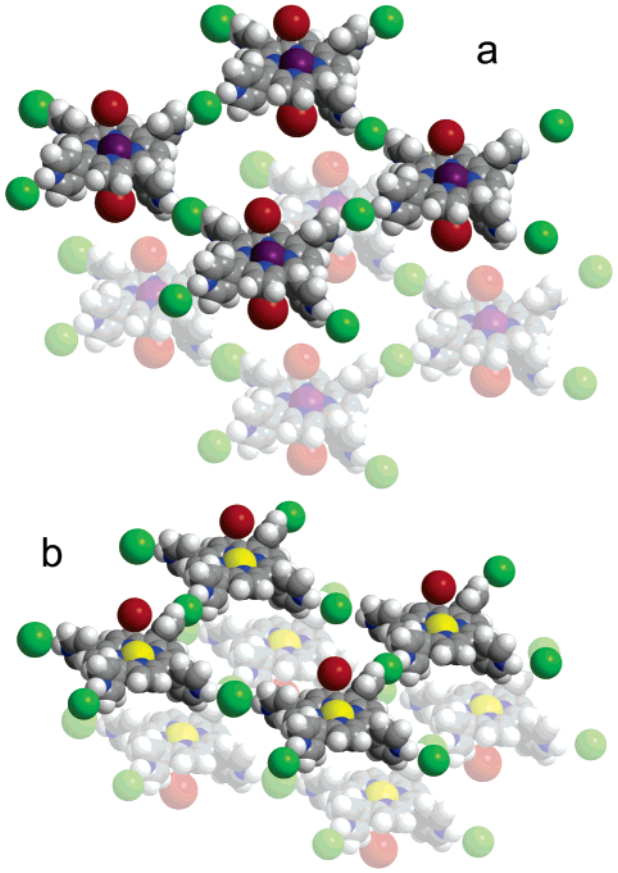

Figure 8. Schematic model of the Mn(III)TpyP(4) (a) and Zn(II)TpyP(4) (b) deposits. The green spheres represent the anions, and the red ones represent the ligands coordinated to the metal ions.

between tetraprotonated TpyP(4) molecules and the relative anions. Indeed, the presence of contacts between chloride anions and peripheral pyridinium groups has already been reported in the crystal structure of the TpyP(4) hexa-acid derivative.[19]

Second, porphyrin core protonation seems not to be sufficient to obtain the formation of deposited samples from dichloromethane, and the presence of *meso* substituents capable of supramolecular interactions appears as necessary for this purpose. In fact, no deposition or aggregation phenomena are observed either for TPP or tetra(4-methoxyphenyl)porphyrin (TMPP), where the hydrogen-bonding ability present in THPP is precluded by substitution of the *p*-hydroxy groups with *p*-methoxy ones. Also in the case of

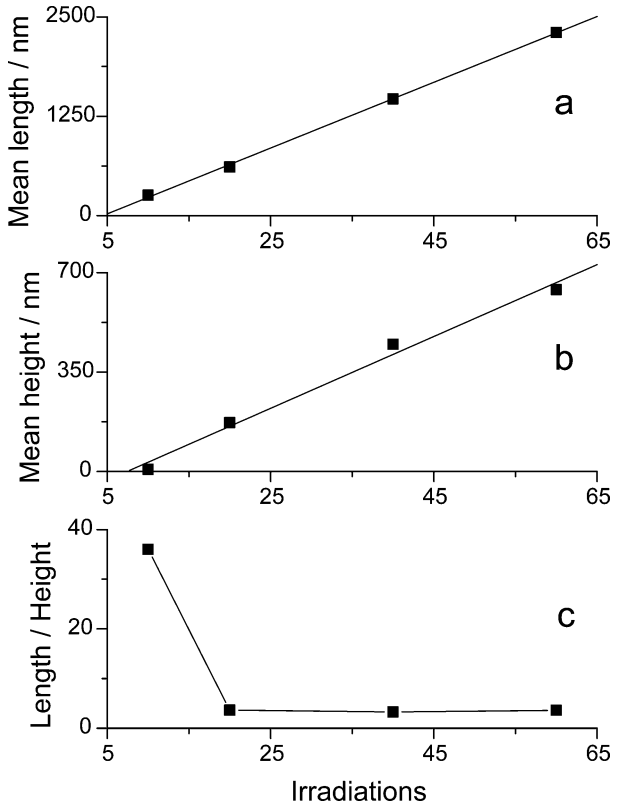

Figure 9. Mean length (a), mean height (b), and length to height ratio (c) of the deposited crystals as a function of the number of irradiations performed for their formation. [TpyP(4)] $\sim$ 6 μM; UV light source: spectrophotometer lamp; i.t. = 0.3 s, d.t. = 15 s. Data obtained from AFM images of the deposited samples.

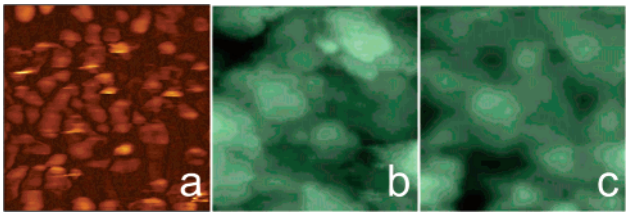

Figure 10. AFM and SNOM images of the nanosized platelets obtained by shortly irradiating a TpyP(4) solution with a spectrophotometer lamp. [TpyP(4)] $\sim$ 6 μM, i.t. = 0.3 s, d.t. = 15 s, t.t. = 150 s (10 pulses). (a) AFM, 2.5 $\times$ 2.5 μm^2. (b) SNOL, topography, 1.5 $\times$ 1.5 μm^2. (c) SNOL, optical image, λ_{exc} = 488 nm, 1.5 $\times$ 1.5 μm^2.

THPP and OHPP, protonation can only occur at the core nitrogen atoms, but the presence of the hydroxyl groups on the *meso*-phenyl rings provides the possibility of hydrogen bonding between the protonated core and the macrocycle periphery.[35] With the three TpyP isomers, the protonation of both the peripheral pyridyl moieties and the core nitrogen atoms is attainable, and solid samples are obtained in the three cases. Anyway, tetraprotonation of the macrocycle periphery seems to be sufficient to allow porphyrin deposition: with the Mn(III) and Zn(II) metal derivatives of TpyP-(4), the formation of solid samples has not been precluded by preventing core protonation via metal ions coordination. The difference of crystal morphology observed in these two latter cases can be possibly ascribed to the different coordination environments for the two metal ions. Stacking interactions are hindered by the presence of two axial ligands in the Mn(III) derivative (hexa-coordinated), while this kind of interaction is still attainable for the Zn(II) complex (penta-

coordinated): in this latter case, a face of the porphyrin macrocycle is still accessible for the interaction with a neighboring molecule. The schematic models proposed for the microcrystals of these species are shown in Figure 8.

Control of Crystal Size. This method of producing assemblies has been further explored to probe the possibility of controlling the size of the deposited crystals and obtaining nanosized porphyrin structures. An AFM study has been carried out on samples deposited on silica by irradiating various aliquots of the same TpyP(4) solution for different total irradiation times (t.t.) (i.e., as a function of the number of light pulses). The analyses of the objects size show that a linear dependence exists between the number of pulses and the mean length or height (Figure 9a and b, respectively) of the deposited crystals. Correspondingly, this dependence can be exploited to control the size of the deposited structures by controlling the number of irradiations, providing a simple and rapid method to generate nanosized porphyrin structures. Indeed, the formation of TpyP(4) nanoplatelets (length, ~257 nm; height, ~7 nm; length to height ratio, ~36; Figure 10) can be observed just after ten irradiations (i.t. = 0.3 s, d.t. = 15 s).

The topography obtained by the SNOL technique shows a number of nanostructured crystals whose shape and size is fully compatible with the AFM data. The fluorescence image, simultaneously collected during the SNOL experiment, is easily interpreted as due to the emission of the porphyrin nanocrystals.

Conclusions

The experimental results of this investigation illustrate the relevant parameters underlying the present method, which easily allows to deposit a variety of porphyrin derivatives by irradiating their solutions in halogenated solvents with a UV light source.[15] This method exploits the slow generation of haloacid in situ due to UV-induced photodecomposition of the solvent,[26] with consequent formation of porphyrin acid derivatives. The low solubility of these protonated species in the organic phase causes the formation of porphyrin nano and microcrystals at the interface between the solvent and the surface hit by the light beam.

It has been elucidated that the nature of the *meso* substituents deeply influences the morphology and optical properties of the deposited samples and even determines the possibility for the deposition to occur. Indeed, only with macrocycles whose periphery is capable of supramolecular interactions, such as electrostatics or hydrogen-bonding, deposition of porphyrins is obtained. Additionally, the morphology and photophysical properties of the deposits can be further modulated by varying the other chemical species involved in the experiments (i.e., the halogenated solvent and the surface) or the experimental conditions such as light source, irradiation time, and delay time. In particular, the monodispersity of the objects dimensions can be favored by maintaining a low local concentration of the photogenerated acid, while their mean size can be varied by changing the number of irradiations performed during the deposition experiment. Finally, the control over this latter parameter has demonstrated the possibility to rapidly deposit fluorescent porphyrin nanoparticles, opening the way to potential nanotechnological applications of this deposition method.

Acknowledgment. The authors thank Dr. Norberto Micali (IPCF-CNR, Messina) for optical microscopy facility and Dr. Anna Bonavita (Università di Messina) for technical assistance with SEM. MIUR (COFIN 2004-06) is acknowledged for financial support.

Supporting Information Available: Spectral changes on irradiating a TPP dichloromethane solution; pictures, extinction, and fluorescence spectra of TpyP(4) deposit on quartz; optical images of TpyP(2) and TpyP(3) solid samples. This material is available free of charge via the Internet at http://pubs.acs.org.

CM060896S